



## **Bachelor Research Project**

Investigating the magnetic properties and the phase transition between  
hydrous and anhydrous phases of anilinium cobalt chloride

**Student:** Aleksandr Igoshin

**Student number:** S3953459

**Supervisor :** Dr. Graeme Blake

**1st Assessor:** Dr. Graeme Blake

**2nd Assessor:** Dr. Beatriz Noheda

**Date of submission:** 23.03.2024



## Abstract

Anilinium cobalt chloride(ACC) is a hybrid perovskite where octahedra of bivalent cobalt hexachloride form linear chains separated by monovalent anilinium cations between the chains. The target compound was synthesized from the anilinium chloride and cobalt (II) chloride hexahydrate precursors by slow crystallization by evaporation from hexan-1-ol or propan-1-ol solvents. Depending on choice of solvents and conditions pink, blue or turquoise phases were synthesized.

The product was characterized by X-ray powder diffraction and Physical Properties Measurement System(PPMS). The pink phase was identified as the hydrated form of the target compound whilst the blue and turquoise phases were shown to have similar crystal structure parameters with different effective magnetic moments and Weiss temperatures as per Vibrating Sample Magnetometer(VSM) data. Said data is analyzed by fitting it to the Curie-Weiss law which yielded Curie constants and Weiss temperatures reflective of the magnetic interactions in the material. Taking into account that the cobalt dication  $\text{Co}^{2+}$  is a  $d^7$  transition metal that can exist in a low or a high spin state( $S=3/2$  and  $S=1/2$ ), the effective moments from Curie constants and  $d^7$  spin states were compared highlighting difference in magnetic configuration of the phases.

The blue phase is synthesized over the turquoise phase in propanol due to the former being more kinetically favorable whilst the turquoise phase is achieved by either prolonged exposure to air or synthesis in hexanol allowing for the most thermodynamically stable phase of ACC to form. Furthermore, exposing the blue phase to UV increases the rate of transition yielding the turquoise phase which could not be reversed to the blue phase by stimuli examined. The transition from the pink phase was achieved by exposing the product to heat, UV or vacuum to dehydrate the product obtaining blue and turquoise phases; whilst obtaining the hydrated phase was done by exposing blue or turquoise phases to water. Nonetheless both the blue and turquoise phases are susceptible to water forming hydrated ACC(HACC). Additionally the target compound was found to degrade after 2 hours of heating to  $90^\circ\text{C}$ .

The reversible transition from pink and blue phase is accompanied by the liberation of water while the irreversible transition from blue to turquoise is highlighted by a change in magnetic properties. Thus (ir)reversibility of transitions along with thermodynamics of the phase formation make anilinium cobalt chloride a potent candidate for investigation to use in photochromic applications.<sup>16</sup>

The anhydrous phases of the material exhibit antiferromagnetism while the hydrated phase is paramagnetic. The transition between the two states is reversible and accompanied by color change from pink to blue / turquoise. Moreover the blue and turquoise phases have different magnetic moments.

## Introduction

The everpresent desire to shift to clean and renewable energy over the last decades drives researchers to explore innovative solutions to generate energy. Semiconductor perovskites are amongst the materials being investigated because of their electronic, magnetic and optical properties. Originally identified in naturally occurring materials, perovskites are a family of crystal structures consisting of a three-dimensional network of metal cations coordinated to anions in an octahedral arrangement.

Some of the key features of perovskites include their intrinsic ability to tolerate defects as a consequence of their three-dimensional network of octahedrons which share cornering anions allowing them to retain the structure in presence of irregularities. Furthermore, the ability to change the composition of the perovskite by changing either cation or anion in crystal lends to an adjustable energy difference between valence and conduction bands optimizing the material to suit a variety of photochromic applications. Particularly, photochromic perovskites with their ability to reversibly change color and absorbance of light offer an extra degree of functionality broadening the range of possible applications.

The material of interest, anilinium cobalt chloride, is a hybrid 1D perovskite exhibiting photochromism. It undergoes a transition from pink to blue to turquoise as induced by exposure to UV or ambient conditions. The transition is accompanied by a change in magnetic properties prompting an investigation into the material magnetic configuration along with reversibility of said transition,

## Target Compound: Anilinium Cobalt Chloride

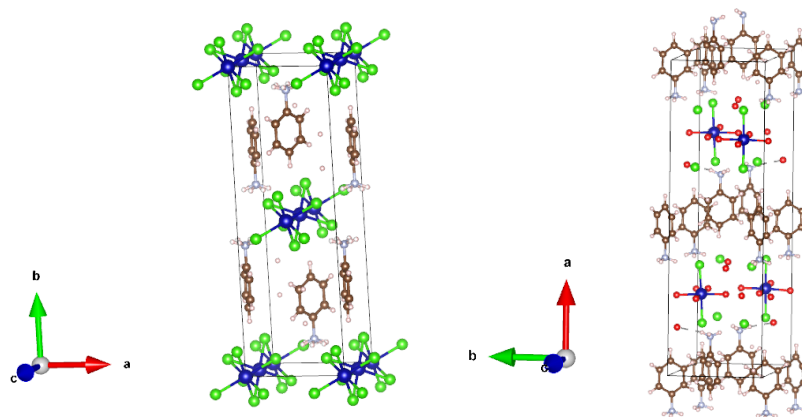


Figure 1: Unit cell structure of anhydrous  $\text{AnCoCl}_3$  (left) and hydrated  $\text{AnCoCl}_4 \cdot 6 \text{H}_2\text{O}$  (right) states of anilinium cobalt chloride, where green atoms are chlorides, blue are cobalt dications, brown are carbons, white are hydrogens and red are oxygens.

Perovskites are a family of crystal structures in the form of  $\text{ABX}_3$  where A and B are cations and X is an anion. In the case of hybrid halide perovskites A is an organic cation, B is an inorganic cation while X is a halide. The target compound,  $\text{AnCoCl}_3$ , is a 1D hybrid perovskite which has two states being orthorhombic anhydrous (ACC) and hydrated (HACC) phases as shown in figure 1 respectively. Upon initial discovery the compound has shown photochromism which warranted investigation on the mechanism by which the material interacts with light and whether said light interactions are responsible



for the phase transition. The transition is accompanied by a change in color from pink to blue and later to turquoise where the first transition is reflective of a change from a paramagnetic to an antiferromagnetic structure.

It was noted upon initial synthesis that while not equally both HACC and ACC respond to ultraviolet light and moisture in air which warranted further investigation of how the external stimuli affected the synthesized material.

### Relevant Theory: Magnetism, Curie-Weiss law and $\mu_{\text{eff}}$

The magnetic properties and phase transition of the target compound, Anilinium Cobalt Chloride, warranted investigation because of the material's ability to change color upon exposure to UV which suggests that it is photochromic as photochromism is a reversible transition between various isomers of a material upon irradiation with only a limited number of materials exhibiting thermally irreversible transitions.<sup>13</sup>

To obtain magnetic properties from the measured magnetisation the magnetic susceptibility  $\chi$  and its inverse  $1/\chi$  are plotted against temperature ranging from 5 K to 300 K. In order to plot said graphs, susceptibility is calculated from magnetisation of the material as measured by VSM. However, as seen in the equation (1) the measured magnetisation is combined from magnetisation from antiferromagnetism along with the diamagnetic contribution from atoms and bonds involved.<sup>1</sup> To calculate said contribution, equation (2) is employed where  $\chi_{\text{atom}}$  and  $\lambda_{\text{bond}}$  are the Pascal's constants.

$$\chi_{\text{sample}} = \chi_{\text{measured}} - \chi_{\text{Diamagnetic}} \quad (1)$$

$$\chi_{\text{Diamagnetic}} = \sum_i \chi_{\text{Diamagnetic, atom, } i} + \sum_i \lambda_{\text{Diamagnetic, bond, } i} \quad (2)$$

With diamagnetic contribution accounted for, the magnetic susceptibility of the material allows the inverse to be found as well. Said values are separately plotted against temperature.

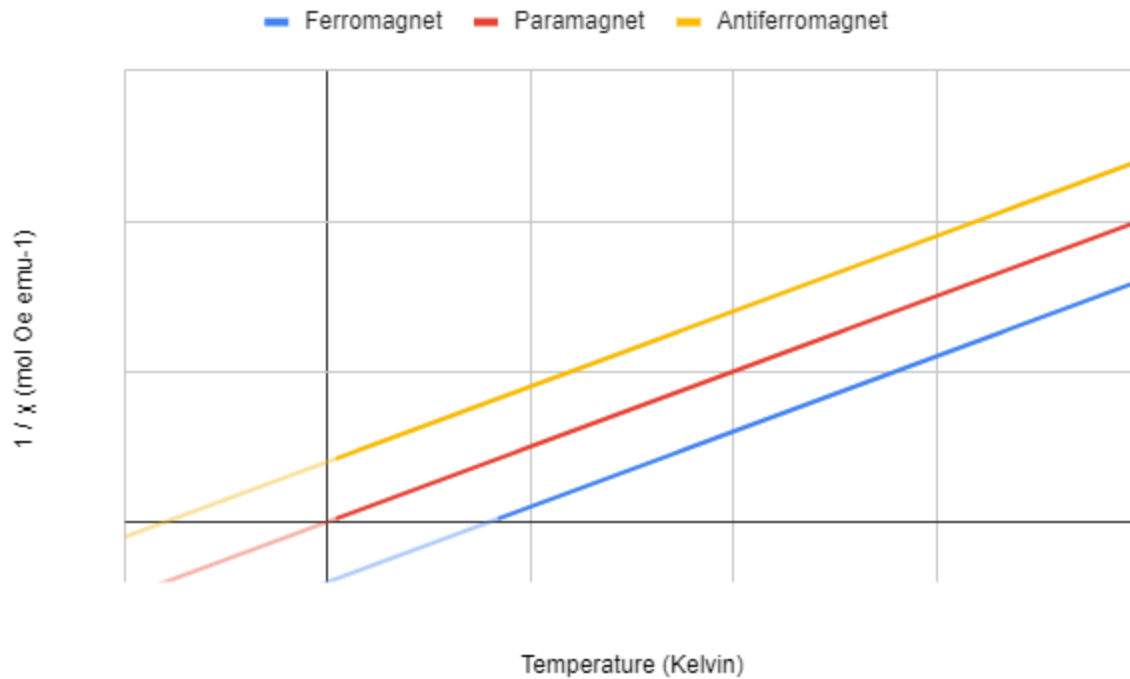


Figure 2: Temperature versus  $1/\chi$  plots for a paramagnet, a ferromagnet, and an antiferromagnet

As seen in Figure 2, if the material is antiferromagnetic, the graph would be a straight line which obeys equation (4) with an x-axis intercept representing  $\frac{\theta}{C}$  where  $\theta$  is the Weiss temperature and  $C$  is the Curie constant.

$$\frac{1}{\chi} = \frac{T}{C} + \frac{\theta}{C} \quad (4)$$

$$\mu_{eff} \cong \sqrt{8 * C}, \text{ unit of } \mu_B / Co^{2+} \quad (5)$$

$$\mu_{eff} = 2 * \sqrt{S * (S + 1)}, \text{ unit of } \mu_B / Co^{2+} \quad (6)$$

The Curie constant is used to approximate the effective magnetic moment  $\mu_{eff}$  of the material using (5). Cobalt cation  $Co^{2+}$  is a  $d^7$  transition metal in octahedral coordination which can exist in a low spin and a high spin state,  $S = \frac{1}{2}$  and  $S = \frac{3}{2}$  respectively. The calculated effective magnetic moments can be used to compare sample measurements from different phases with spin-only effective magnetic moments to analyze how changes in structure affect the magnetic configuration. Assuming that the orbital moment can be neglected, the effective magnetic moment can be approximated using equation (6).



## Materials and Methods

### Materials used

**Cobalt (II) Chloride Hexahydrate(CCH)** - is hydrated cobalt dichloride coordinated to 6n water molecules for n atoms of cobalt. CCH is a purple powder that acts as an allergen meanwhile having a high affinity for water meaning that it should be dehydrated and kept under argon; since given time it will absorb the moisture from air within hours.

**Anilinium chloride(AC)** - is the precursor to the organic cation, anilinium, in the hybrid perovskite product. It is a white powder which does not absorb water as readily as CCH but nonetheless it is dehydrated each time before use. A molar excess of AC is used (1.5 mol AC : 1 mol CCH) because an organic impurity will not have as much of an effect on the electronic/magnetic properties of the material as a cobalt impurity.

### Choice of solvent and additives

**Ethanol:** was chosen because of its availability and ability to dissolve the precursors at room temperature with minimal stirring. Furthermore, with a low boiling point of 78 °C it is volatile thus permitting isolation of product by evaporation.

**Propan-1-ol:** Considering that the initial objective is to synthesize only the blue phase of ACC, propan-1-ol was chosen for its relatively low steric effect in comparison to hexan-1-ol, such that the shape of the former allows for better reactivity because of the smaller size.<sup>5</sup> Consequently, other adjustments to the setup are necessary to increase the grain size. Propanol does not dissolve the precursors as effectively as ethanol at r.t.; however, given 30 min at 35 °C all precursors dissolve without inducing significant evaporation of the solvents. Should it be necessary a 1:1 mixture of hexan-1-ol and propan-1-ol would be used to increase the grain size.

## Methods

### Experiment 1. Crystallization by solvent evaporation in air at r.t.

Initially a mixture of target compounds (HACC and ACC) were synthesized by dissolving 0.3 mmol of  $\text{CoCl}_2 \cdot 6 \text{H}_2\text{O}$  and 0.3 mmol of anilinium chloride in 6 ml of ethanol in a vial equipped with a stirring bar. After 15 min the precursors were fully dissolved, the stirring was stopped and the vial was covered with parafilm. Following that holes were punctured in film and the mixture was left for 1 day until the solvent had evaporated. The resultant product was a dispersed mixture of pink and blue phases.

### Experiment 2. Antisolvent Volatilization Crystallization of ACC using Ethanol : X in air at r.t. (X = Acetonitrile, Toluene, Diethyl ether)

In an effort to increase conversion of precursors and favorability of single phase synthesis an antisolvent volatilization crystallization approach was chosen with a variety of possible antisolvents.<sup>10,17,21,26,29</sup> In this case, the antisolvent is an additive solvent which decreases solubility of the product facilitating synthesis

of crystals.<sup>7</sup> To test the viability of toluene, acetonitrile, and diethyl ether a simple antisolvent setup was used. Equimolar amounts (0.3 mmol) of hydrated cobalt chloride and anilinium chloride per batch were transferred to a vial. A total of three batches were made to test three antisolvents separately. Subsequently 6 ml of ethanol were added to each vial and using a stirring bar the vials were left stirring for 5 min at 200 rpm until the precursors had dissolved. Consequently the stirring was stopped and 6 ml of an antisolvent were added to the setup. The vials were covered with parafilm with holes and then were left for a day to allow the solvent to evaporate at a low rate. Once ethanol has evaporated it became apparent that little to no crystallization has occurred highlighting that either the antisolvent choice and/or the setup used were flawed.

Given lack of crystallization, a reverse addition approach was used by using the same equimolar amounts in 6 ml of ethanol in small vials which were then submerged in larger vessels filled with 6 ml of chosen antisolvents (toluene, acetonitrile and diethyl ether) and subsequently covered with caps. Leaving the vessels undisturbed for a week yielded no tangible crystallization which is likely a result of ethanol's volatility hindering the formation and stabilization of the nucleation sites.

### Experiment 3. Synthesis of ACC by solvent evaporation under argon at r.t.

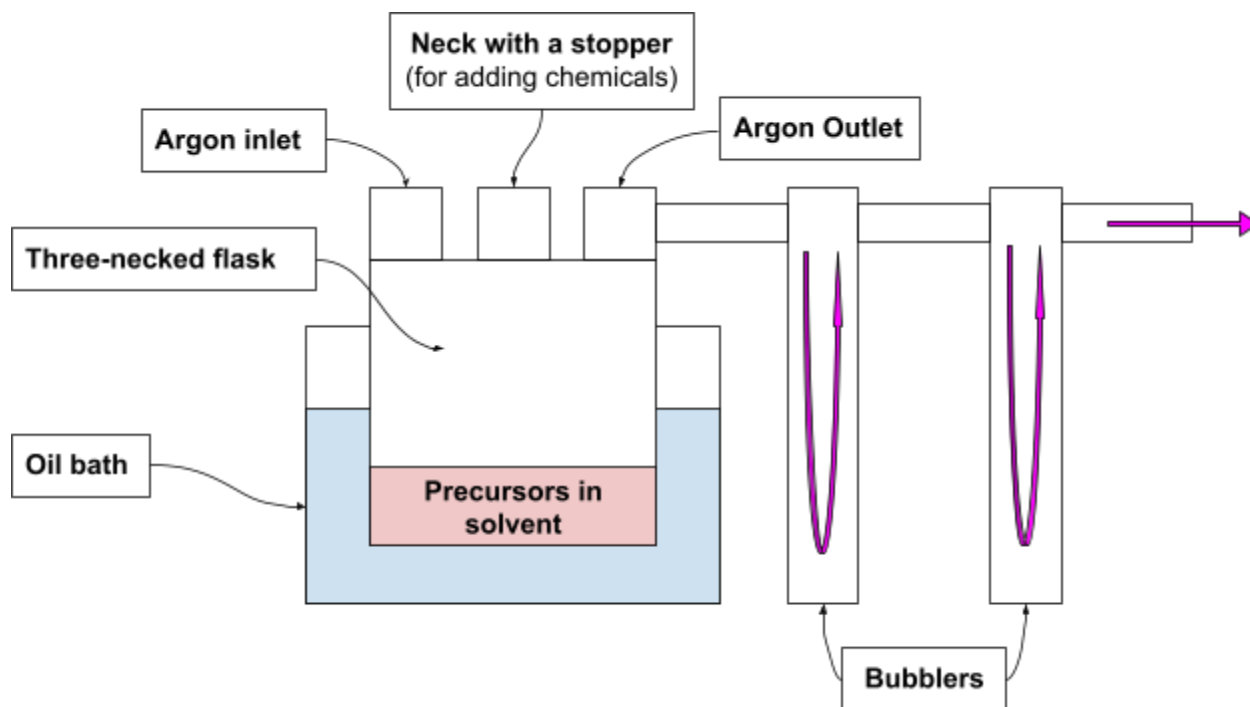


Figure 3: Schematic representation of the setup used in experiment 3 and 4, where the three-necked flask was moved up out of the oil bath after dehydration of precursors.

In an effort to minimize the effect of moisture in air on the crystallization, the setup was modified to run under argon as shown in figure 3. Prior to addition of precursors to the vial, the system was purged of oxygen and then equimolar amounts (0.3 mmol) of  $\text{CoCl}_2 \cdot 6 \text{H}_2\text{O}$  and anilinium chloride were added through the top neck of the flask without turning off the argon supply. Adding 4 ml of ethanol and ensuring that the precursors were dissolved, the mixture was left under argon overnight. The resultant product showed that evaporation was accelerated due to a continuous stream of argon leading the cobalt



chloride to reform. Hence prompting a repeat of the experiment with a lower rate of gas supply which yielded a mixture of HACC/ACC suggesting that water coordinated to cobalt chloride has an effect on the products formed as any gaseous water in the vessel would be removed with Argon.

#### **Experiment 4. Dehydration of precursors and subsequent synthesis of ACC under Argon in a variety of solvents (EtOH, PropOH, HexOH)**

To selectively synthesize ACC over HACC, a setup from a previous experiment was modified to reduce the amount of water in the system. Initially the system was purged with argon and 0.3 mmol of cobalt chloride were added to the flask which was submerged in an oil bath. The bath was heated to 250 °C and cobalt chloride was left to be dehydrated for 2 hours. Subsequently, after the heating was turned off and once cobalt chloride reached r.t. 0.3 mmol of anilinium chloride was added. The precursors were dissolved in 4 ml of 1:1 EtOH/PropOH mixture and the mixture was stirred until the reagents dissolved. Leaving the mixture for two days under low gas supply allowed both alcohols to evaporate yielding a blue crystalline product.

To avoid having cobalt chloride impurities in the final material, an excess of anilinium chloride was used (0.45 mmol). Using the same setup as prior, before adding the solvent the anilinium chloride was dehydrated in the three-necked flask with already dehydrated cobalt chloride still inside by heating the system to 100 °C using an oil bath and keeping it at said temperature for 1 hour. Furthermore 3 ml of 1:1 the ethanol/propanol mixture was used instead of 4 ml which has yielded smaller blue crystals in comparison to using larger amounts of solvent.

Using exclusively 4 ml of propanol as a solvent increased the time taken for crystallization because of its lower volatility than ethanol. Despite propanol taking longer to evaporate than ethanol, the grain size of the product formed has increased as precursors have more time to congregate in a favorable manner. Lastly, using 4 ml of hexanol instead of propanol could further improve the selectivity of which phase forms allowing turquoise phase to form using the same setup as shown in figure 3.

#### **Experiment 5. Synthesis of hydrated ACC(HACC) by water evaporation in air**

In an attempt to have HACC be the main product of the reaction, the setup from experiment 1 was used with water instead of ethanol as solvent. Neither of the precursors were dehydrated in order to shift the favorability of the reaction towards the hydrated product. The precursors were dissolved in water at r.t. Using a stirring bar at 300 rpm and subsequently the stirring was stopped and the mixture was heated to 50 °C to promote evaporation of water. After leaving the setup overnight, the product was obtained as large pink crystals and powder of blue and turquoise phases.

#### **Analytical techniques. X-Ray diffraction and Vibrating Sample Magnetometer**

In an effort to identify which of the pink, blue and turquoise phases exist in a hydrated or an anhydrous state, the solved crystal structures had XRD patterns approximated using Vesta.<sup>19</sup> Utilizing Profex, these patterns would be compared to patterns obtained with X-Ray Powder Diffraction allowing to identify phases formed and approximate composition of the product giving insight on the mechanism by which transition occurs and the efficiency of the synthetic approach used.<sup>8</sup>



Utilizing the Physical Properties Measurement System (PPMS), particularly the Vibrating Sample Magnetometer (VSM), the measurement was conducted from 5 to 300 Kelvin without a field and with a field of 1000 Oersted.<sup>22</sup> Thus the effective magnetic moments and Weiss temperatures of the samples could be probed which are representative of the strength of magnetic interactions in blue and turquoise phases shining a spotlight on the mechanism of the transition and potential differences between two phases.

## Results and Discussion

### Microscope findings



Figure 4: Photo of a split pink phase crystal of sample 1 from Experiment 1 upon exposure to a UV lamp at 20% for 30 min showing a change in color on the outside of the crystal from pink to turquoise

The crystallization by solvent evaporation in air yielded a mixture of products. Under the microscope a dispersed mixture of pink and blue phases were identified. Exposing sample 1 to a UV lamp at 20% of the maximum power for 1 min induced a phase change as both phases began to change color; although they did so unevenly with the pink phase exhibiting the most change gradually becoming blue. Upon exposing part of the pink phase of sample 1 to a UV lamp at 20% for 30 min the phase began to change color to turquoise as seen in figure 4. After leaving an unexposed portion of the product in the dark for 2 weeks, the powder has turned completely turquoise implying that either exposure to air or time have induced the same phase transition as exposure to UV. Following the controlled solvent evaporation crystallization under argon in experiment 3, the product obtained was majorly the blue phase with pink being the minor product. Exposing the powder to the UV lamp at 20% for 30 min yielded the same result as before turning the powder turquoise. In experiment 4 using 1:1 mixture of ethanol/propanol during solvent evaporation synthesis yielded a product, majority of which was the blue phase. After exposing sample 4 to UV, the powder turned turquoise. Subsequently after selectively synthesizing the turquoise phase it was observed under a microscope to compare with previous samples exposed to UV to gauge whether the turquoise phase synthesized is the same as that yielded by exposure of blue phase to UV.

## Characterisation by X-Ray powder diffraction

In an effort to verify the findings under microscope, the following XRD measurements were performed from  $5^\circ$  to  $50^\circ$  in  $0.02$  increments at  $30$  rotations of the sample holder per minute. The sample was fixed to a zero-background sample holder using a minimal amount of grease to avoid uneven distribution of the powder hindering the data.

### Experiment 1: Crystallization by solvent evaporation in air at r.t. Sample 1

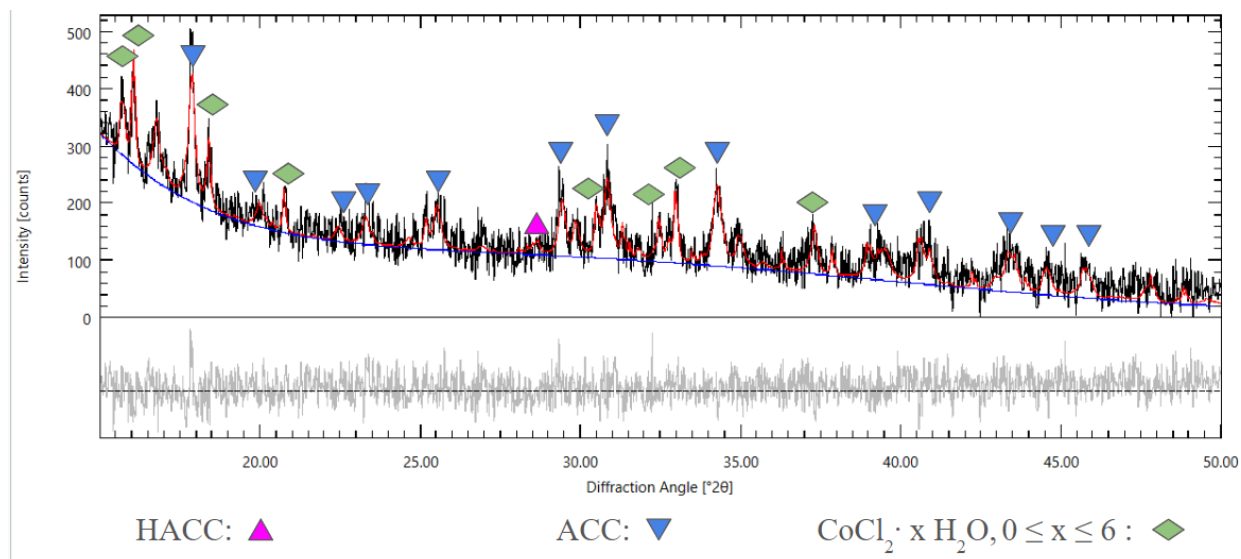


Figure 5: XRPD pattern of pink/blue sample as obtained solvent evaporation in air at r.t., where the black line is the measured data, blue line is the fitted background, red line is a fit to the pattern all for sample 1 and the gray line is the difference profile for sample 1 (Refer to Experiment 1, Sample 1 in the appendix for refined cell parameters)

Powder X-ray Diffraction was done on the product obtained by simple solvent evaporation crystallization in air. Utilizing the crystal structures solved in previous work using single-crystal XRD, a powder XRD pattern was simulated using Vesta to compare it with the XRD data obtained that was then analyzed in Profex.<sup>8</sup> The refinement done on the data has shown that  $70$  wt% is ACC,  $4$  wt% is HACC whilst  $26$  wt% is the hydrated cobalt chloride precursor. As seen in figure 5, the peaks labeled blue are attributed to ACC while the weak peak labeled pink is caused by HACC allowing distinguish which of the phases have formed. The synthesis has not reached completion as a large amount of precursor still remained whilst yielding a mixture of two phases of the target compound suggesting that the synthesis in air was to be tuned to ensure better conversion of precursors to the final product and that the product formed was primarily a single phase. Comparing the data with examination of the sample under the microscope suggests the blue phase is the anhydrous phase of ACC whilst the pink phase, in this case, is a mixture of cobalt chloride and the hydrated phase of the material.

**Experiment 2:** Antisolvent Volatilization Crystallization of ACC using Ethanol : X in air at r.t. (X = Acetonitrile, Toluene, Diethyl ether) Sample 2 and 3

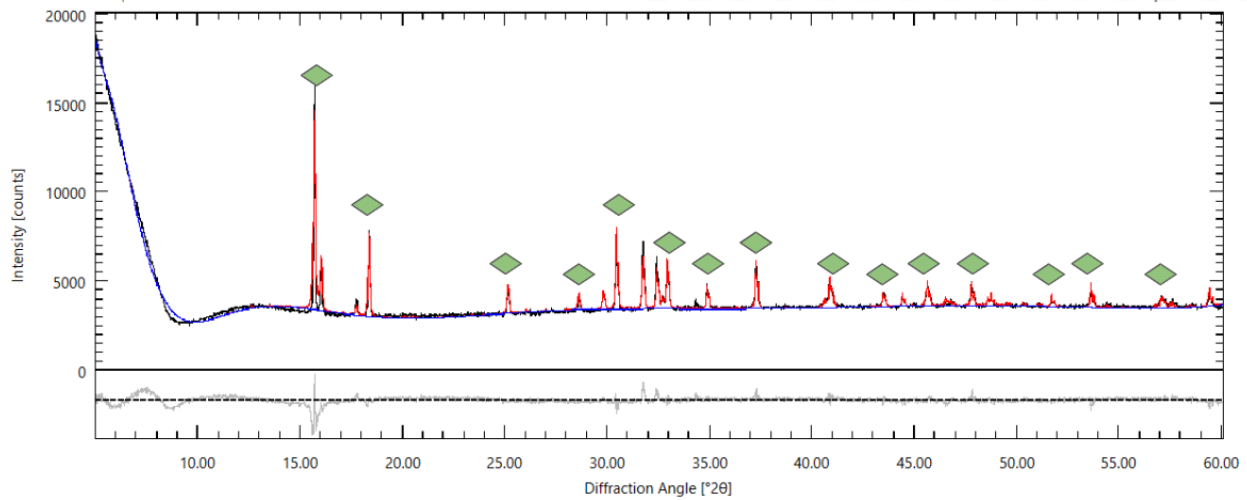


Figure 6: XRPD pattern of cobalt chloride crystals reformed during AVC with EtOH:ACN, where the black line is the measured data, blue line is the fitted background, red line is a fit to the pattern all for sample 2 and the gray line is the difference profile for sample 2 (Refer to Experiment 2, Sample 2 in the appendix for refined cell parameters)

The XRD pattern in figure 6 was obtained from the sample 2 synthesized by antisolvent volatilization crystallization (AVC) with ethanol acting as the solvent and acetonitrile as the antisolvent. All of the pronounced peaks labeled green are characteristic to cobalt chloride. The refinement has shown that the majority of the product (96 wt%) is the cobalt chloride precursor and the rest is HACC (4 wt%) whilst no ACC was formed. The poor conversion of the precursor to product could be attributed to volatility of the solvent and antisolvent used failing to sustain nucleation sites for crystallization. Furthermore, acetonitrile and ethanol are miscible with each other which hindered the synthesis whilst the water from air and the hydrated form of cobalt chloride promoted formation of HACC rather than ACC.

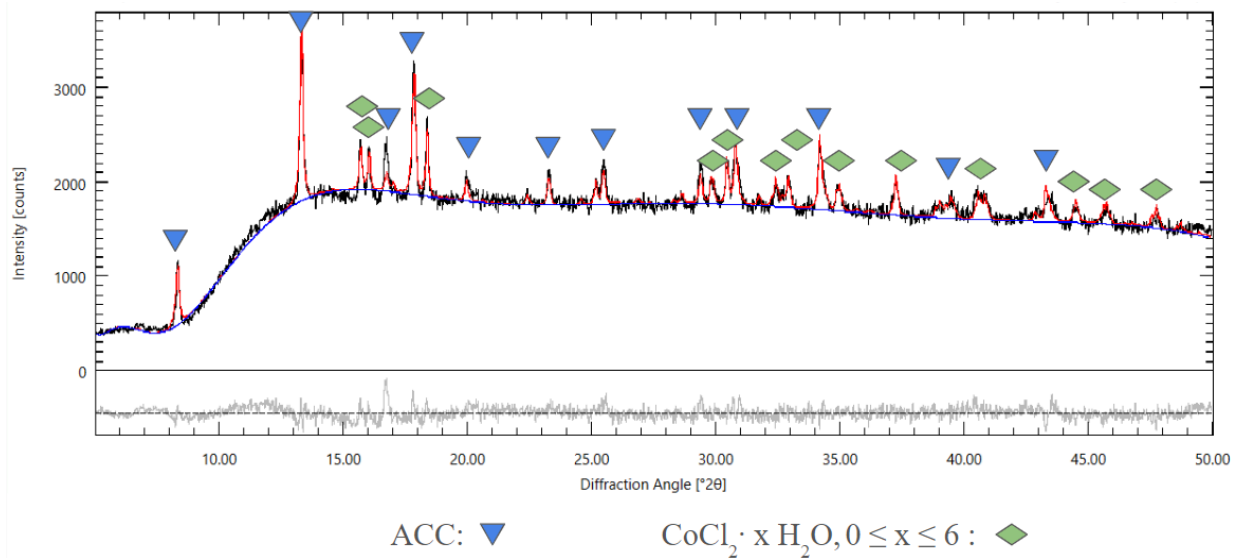


Figure 7: XRPD pattern of blue crystals obtained through AVC with EtOH:Toluene, where the black line is the measured data, blue line is the fitted background, red line is a fit to the pattern all for sample 3 and the gray line is the difference profile for sample 3 (Refer to Experiment 2, Sample 3 in the appendix for refined cell parameters)

The sample 3 obtained using a solvent:antisolvent system with ethanol:toluene yielded blue crystals of a small grain size. As seen in figure 7, the peaks labeled blue are indicative of ACC present in the sample whilst the extra peaks labeled green show that cobalt chloride precursor is present in the sample implying that conversion has not reached completion. The refined composition of the sample has shown that 68 wt% is ACC, 3 wt% is HACC, and 29 wt% is the cobalt chloride precursor. Given the outcome of the crystallization by solvent evaporation in air and antisolvent volatilization approaches, an excess of the other precursor, anilinium chloride, should be used to provide better conversion of cobalt chloride as the latter has a magnetic moment which would affect the results from VSM.

**Experiment 4:** Dehydration of precursors and subsequent synthesis of ACC under Argon in a variety of solvents (EtOH, PropOH, HexOH). Samples 4-6

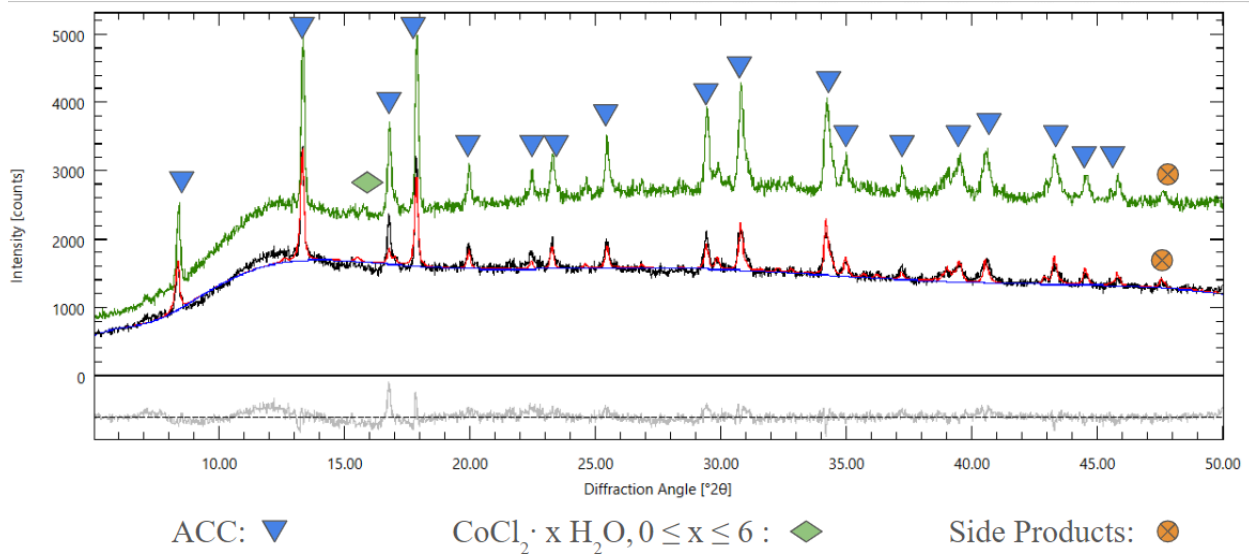


Figure 8: Overlaid XRPD patterns of blue ACC by solvent evaporation before (bottom) and after (top) exposure to UV, where the black line is the measured data, blue line is the fitted background, red line is a fit to the pattern all for sample 4, the green line is the XRD pattern for sample 5 and the gray line is the difference profile for sample 4 (Refer to Experiment 4, Sample 4 and 5 in the appendix for refined cell parameters)

The product was obtained by dehydration of precursors and subsequent crystallization by solvent evaporation under Argon using a 1:1 mixture of ethanol:propanol. The overlaid XRD patterns in figure 8 show the same product before (sample 4) and after (sample 5) exposure to a UV chamber at 20% for 1 hour; where the bottom plot is before exposure and top is after exposure. It can be seen from the peaks that ACC is the major product. The refinement indicated that no HACC was formed highlighting the impact of dehydrating the samples along with working under argon on promoting the formation of the anhydrous phase. The composition of the samples before and after UV exposure showed that 93 wt% and 95 wt% is ACC respectively. However, prior to UV exposure there was 3.00 wt% of cobalt chloride present in the sample which was no longer present after exposure that is attributed to poor approximation of the background by Profex. The remainders of the compositions for samples 4 and 5 were refined to have 4 wt% and 5 wt% of side products which were identified as various oxides of cobalt. Using an excess of anilinium chloride has yielded near complete conversion of cobalt chloride in turn increasing the amount of ACC formed.

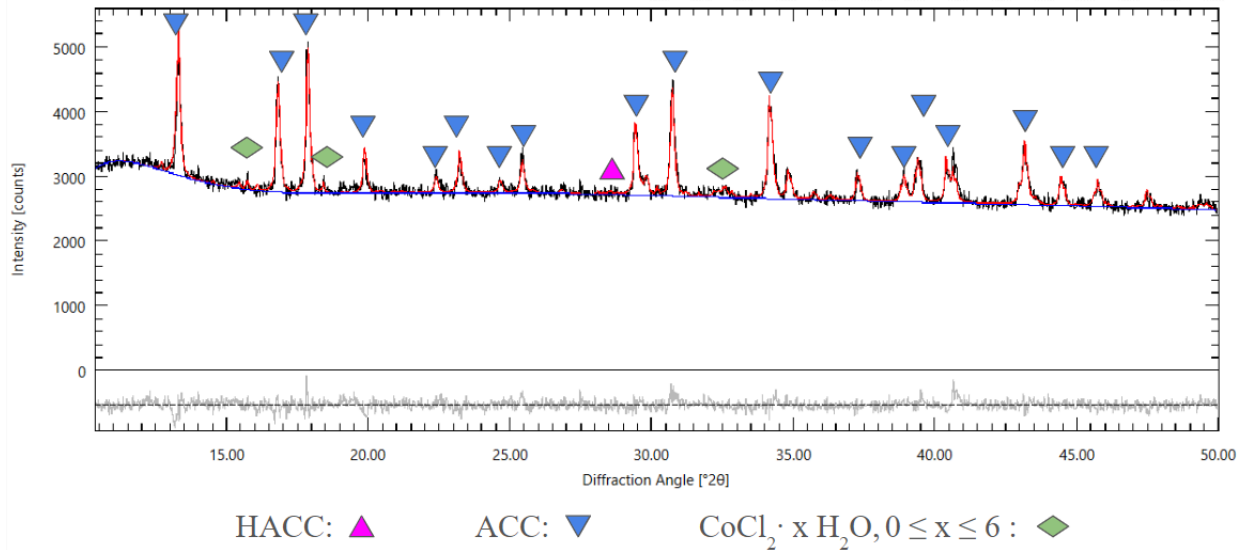


Figure 9: XRPD pattern of turquoise ACC by solvent evaporation (HexOH:PropOH), where the black line is the measured data, blue line is the fitted background, red line is a fit to the pattern all for sample 6 and the gray line is the difference profile for sample 6 (Refer to Experiment 4, Sample 6 in the appendix for refined cell parameters)

To further increase the grain size, 4 ml of hexanol were used; though, due to its inability to dissolve anilinium chloride, propanol had to be added yielding 8 ml of a 1:1 propanol/hexanol mixture. Hexanol being less volatile than other solvents tested increased the evaporation stage of the synthesis to last a week, hence increasing the crystallization time. After 2-3 days after the start of evaporation, the solution turned green implying that while dissolved the material has undergone a transition to the turquoise phase. Thus, using a mixture of hexanol and propanol allowed for selective synthesis of the turquoise phase. As seen in figure 9, the peaks labeled blue suggest that ACC is the major product coinciding with the findings from previous measurements on the blue phase. Additionally a single peak labeled pink is indicative of a small amount of HACC formed whilst the remaining peaks labeled green highlight that the conversion is not entirely complete. Upon refinement it became apparent that the cell parameters for ACC of the turquoise phase (sample 6) are marginally different from ACC of the blue phase (sample 4), as seen in appendix 1 samples 4 and 6, implying that it is the structural changes that are responsible for the color change prompting use of the PPMS machine to perform VSM to probe the magnetic properties of the phases.

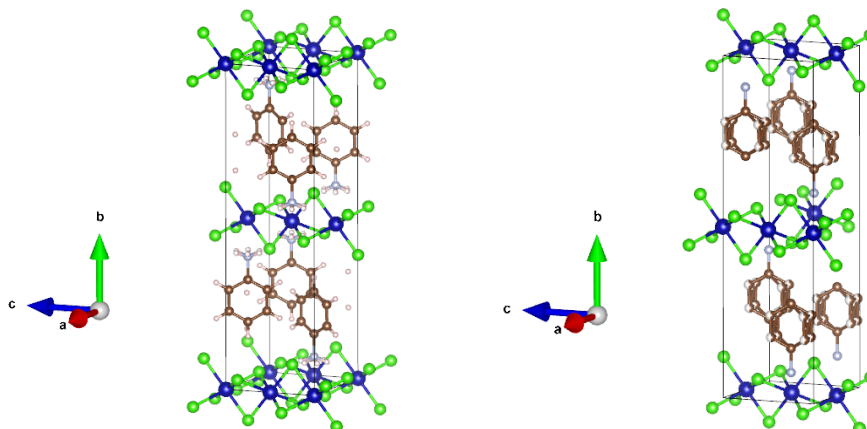


Figure 10: Solved crystal structures of blue(left) and turquoise(right) phases of AnCoCl<sub>3</sub>, where green atoms are chlorides, blue are cobalt dications, brown are carbons and white are hydrogens

As demonstrated in figure 10, solving the crystal structure indicated that the anilinium cations are ordered for the blue phase and disordered for the turquoise phase which are responsible for the change from primitive orthorhombic to C-centered orthorhombic. The refined composition of the product was calculated to be 92 wt% ACC and 8 wt% cobalt oxides.

#### Experiment 5: Synthesis of hydrated ACC(HACC) by water evaporation in air. Samples 7-9

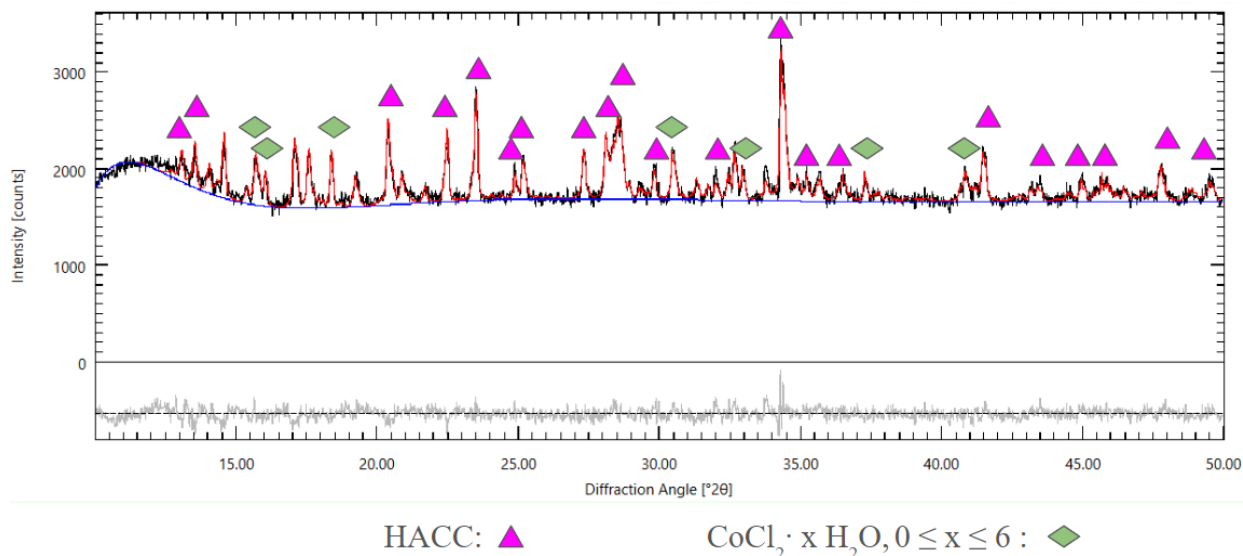


Figure 11: XRPD pattern of the rehydrated ACC, where the black line is the measured data, blue line is the fitted background, red line is a fit to the pattern all for sample 7 and the gray line is the difference profile for sample 7 (Refer to Experiment 5, Sample 7 in the appendix for refined cell parameters)

In an effort to test the reversibility of the transition between HACC and ACC, samples 4 and 6 from experiment 4 were transferred to a glass vial to which a drop of water was added. Upon mixing the powder, it changed from a mixture of blue and turquoise to pink yielding a rehydrated sample. The XRD pattern in figure 11 was obtained using said rehydrated sample. The peaks labeled pink show that HACC was obtained. The refined composition has 97 wt% of HACC and 3 wt% of various cobalt oxides. The



major product being HACC implies that the transition between HACC and ACC is reversible despite ACC being more thermodynamically stable as over time in air the pink phase transitions to blue. In order to further verify said hypothesis the synthesis approach is to be modified to obtain HACC as the majority product. The refined cell parameters for HACC are in agreement with the cell parameters obtained in previous measurements highlighting the ability of compounds to convert between different crystal structures while liberating/incorporating water. Lastly, a portion of sample 7 was placed inside a glovebox where it immediately transitioned to the blue phase inside the evacuation chamber. This observation suggests that while performing magnetic measurements in PPMS the vacuum inside the chamber would induce a transition; hence preventing measurements on the pink phase from being done.

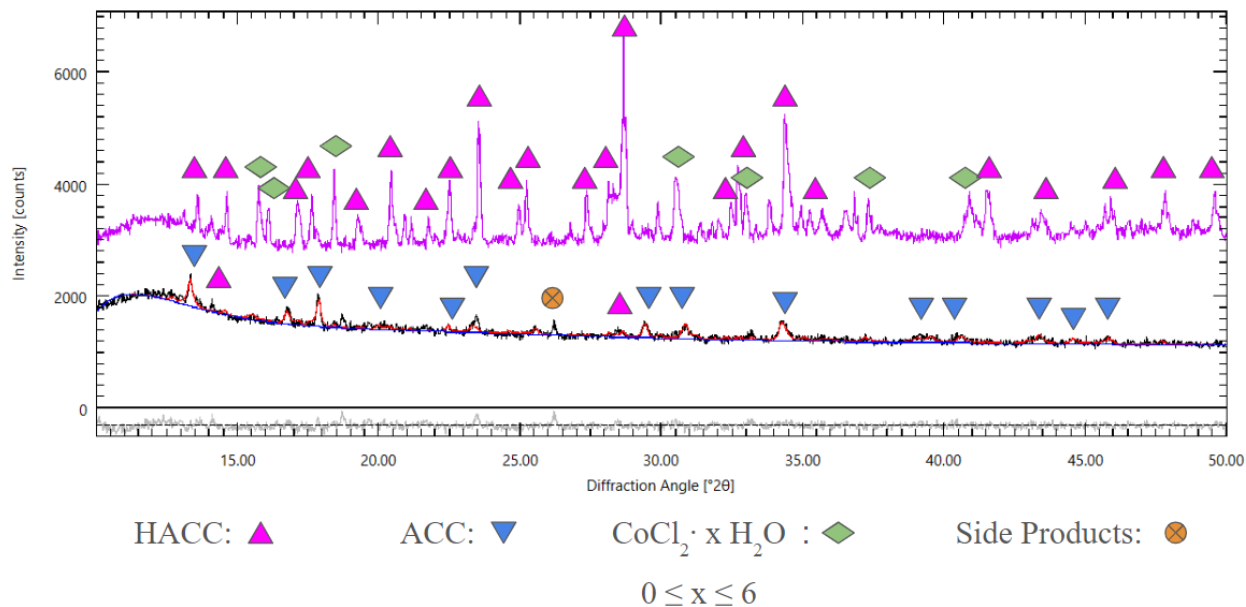


Figure 12: Overlaid XRPD patterns of hydrated ACC before(top) and after(bottom) exposure to UV, where the black line is the measured data, blue line is the fitted background, red line is a fit to the pattern for sample 9 and pink line is the XRD pattern for sample 8 for comparison whilst the gray line is the difference profile for sample 9.(Refer to Experiment 5, Samples 8-9 in the appendix for refined cell parameters)

To intentionally synthesize HACC, the synthesis was performed in air using water as the solvent. Through water evaporation for a day the product was obtained primarily as HACC(Sample 8). Following that, the sample was exposed to UV to test whether the transition from pink to blue phase is accompanied by evaporation of water from the sample. In other words, the changes in structure were probed by XRD to see whether exposing a sample to UV liberates water from the structure yielding ACC(blue). While the conversion from HACC to ACC was not complete, exposing sample 8 to a UV chamber at 30% for 30 minutes induced a transition to blue ACC yielding sample 9 which supports the hypothesis that the phase transition from pink to blue phase is reflective of a change in structure by water liberation. As seen in figure 12, the overlaid patterns of samples 8 and 9 where the top plot is primarily HACC whilst the bottom one is a HACC:ACC mixture respectively. The peaks labeled pink indicate HACC as the major product. In contrast, the bottom plot shows that upon exposure to UV the majority of the product has transitioned from HACC to ACC as illustrated by the majority of peaks labeled blue being caused by ACC rather than HACC. The refined composition of both samples were approximated to be 78 wt% HACC, 2 wt% ACC and 20 wt% various hydrates of  $\text{CoCl}_2$  in the former case whilst being 25 wt%





HACC, 65 wt% ACC and 10 wt% various hydrates of  $\text{CoCl}_2$  in the latter. Based on the refined composition, the contribution from cobalt chloride precursors in sample 9 seems to have decreased upon irradiation by UV which is attributed to poor approximation by Profex as a result of the bottom pattern having peaks notably weaker than for sample 8.

As shown in figure 11, reintroducing water to a mixture of blue and turquoise phases yielded a phase transition from anhydrous crystalline back to the hydrated crystalline phase indicating that the first transition is reversible. Hence, an experiment was conducted to determine whether the turquoise phase can transition back to the blue phase without going through the rehydration step. Neither UV exposure nor temperature were able to induce such change.

Without dehydration the water present in both precursors could be enough to induce formation of HACC; thus making the synthesis less selective. While a complete dehydration of metal halides is a slow process without the use of extra chemicals, it is possible to remove most of the water from the material by heating it.<sup>4,14,18,24</sup> According to research, on average  $\text{MgCl}_2 \cdot 6 \text{H}_2\text{O}$  loses around 4-5 moles of water by heating it to  $120^\circ\text{C}$  from 2 to 20 hours.<sup>27</sup> Employing the same approach for cobalt chloride allowed the powder to be temporarily partially dehydrated provided the air is purged from the system using argon at  $250^\circ\text{C}$ .<sup>18</sup> The dehydration process is accompanied by a change in color from purple to blue acting as a visual indication of the process. With the approach kept the same for dehydrating cobalt chloride hexahydrate, anilinium chloride could also contain some water, but due to it containing an organic component (anilinium), the procedure was adjusted to first remove water from cobalt chloride at  $250^\circ\text{C}$ . Subsequently allowing the mixture to cool down to r.t and then transferring anilinium chloride to the reaction medium and heating the flask to  $100^\circ\text{C}$ . A lower temperature for dehydration was chosen in order to avoid destroying the precursor.

According to research primary alcohols when used as an additive have an effect on the resultant grain size of the crystals.<sup>9</sup> As the length of the alkyl chain increases so does the grain size of crystals formed. Since primary alcohols coordinate the clusters of crystals, an increase in alkyl chain length increases the probable cluster size when grown in solution. Out of the alcohols studied (propanol, butanol, pentanol and hexanol) hexan-1-ol yielded the largest grain size. However, the longer the alkyl chain the less volatile the alcohol is, increasing the time needed for crystallization by evaporation to reach completion.

In contrast to the positive relationship between alkyl chain length in primary alcohols and the grain size of crystals formed, the chain length has a negative relationship with destabilizing metal chloride hydrates. This is due to an increase in the steric effect with increase in chain length making it more difficult for the alcohols to penetrate the hydrate coordinates of the metal halides; hence having less of an effect on the metal halides affinity for water.<sup>12,25</sup>

By taking into account primary alcohols' positive relationship between alkyl chain length and grain size of crystals formed along with their negative relationship between steric effect and destabilizing metal chlorides affinity for water, the choice of alcohols can be adjusted to selectively synthesized blue or turquoise phases. Volatility of solvent has a direct relationship with crystallization time such that hexanol taking more time to evaporate than propanol increases crystallization time yielding the turquoise phase. As such turquoise is the more thermodynamically stable phase. However, hexanol's poor ability to

dissolve anilinium chloride prevents from using it exclusively meaning that a mixture of propanol:hexanol should be used to produce turquoise phase as the major product. In contrast, using only propanol provides a shorter time span for crystallization promoting formation of the more kinetically favorable phase. Propanol's ability to dissolve the precursors with minimum heat, destabilizing effect on the metal chloride hydrates along with lower volatility than hexanol lead to selective synthesis of the blue phase. Lastly, synthesis of the hydrated phase can be done by using water as the solvent; thus granting an excess of it to the system. By doing so and also allowing the water to evaporate slowly in air the hydrated pink phase can be obtained exclusively.

### Magnetic Properties

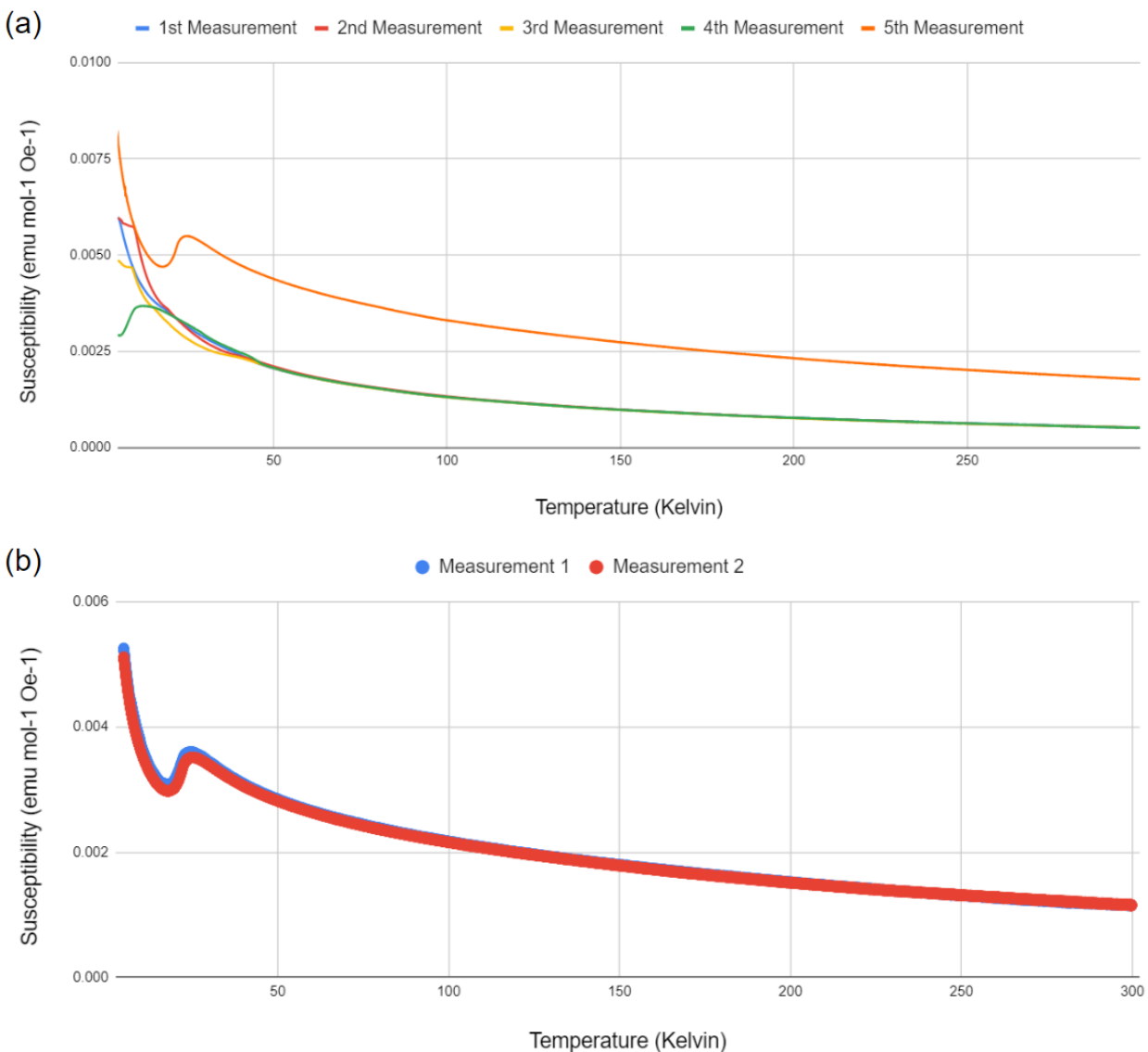


Figure 13: Magnetic susceptibility  $\chi$  versus Temperature plots for (a) blue and (b) turquoise phases exhibiting antiferromagnetic behavior. (b) has a maximum at low temperatures not present in the first 4 measurements in (a).

Upon obtaining VSM data for sample 4 and 6, the susceptibility was calculated as described in the theory section in introduction. Said susceptibility values were plotted against temperature yielding plots shown in figure 13. At low temperatures, plots for sample 4 and sample 6 have a paramagnetic region, where the alignment of moments is not perfect at normal applied fields which is accounted for when using the Curie-Weiss law. Notably, 5th measurement for sample 4 and along with measurements for sample 6 have a maximum at 29 K and 25 K respectively. To approximate the effective magnetic moments for samples 4 and 6, an inverse of susceptibility was calculated and plotted against temperature.

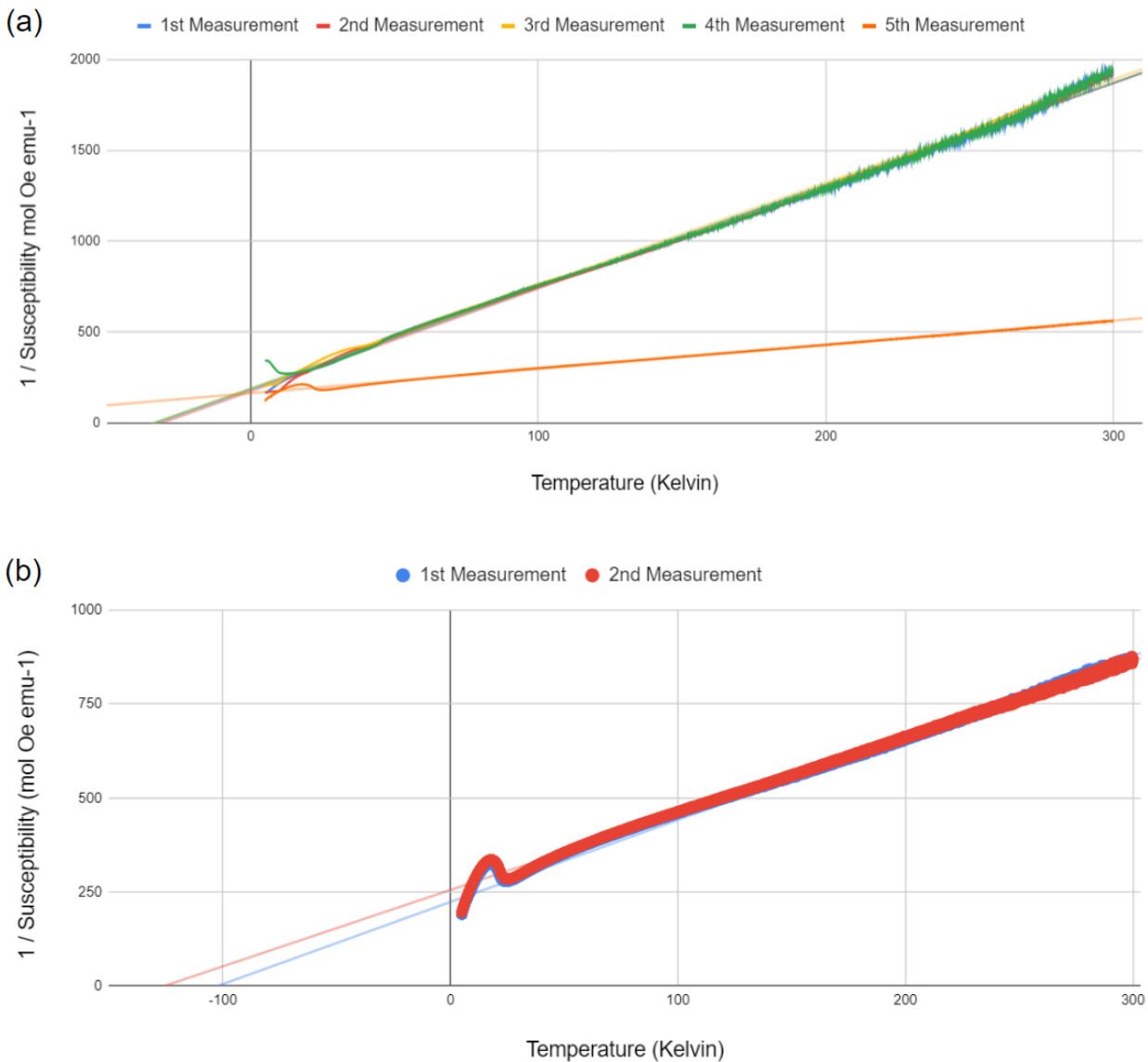


Figure 14: Inverse of magnetic susceptibility  $1/\chi$  versus Temperature plots for (a) blue and (b) turquoise phases exhibiting antiferromagnetic behavior. (b) has a maximum at low temperatures not present in (a)

Both blue phase(experiment 4, sample 4) and turquoise phase(experiment 4, sample 6) exhibit antiferromagnetic behavior as the  $1/\chi$  vs temperature graph yielded a straight line for both as seen in figure 14. The Weiss temperature ( $\Theta$ ) for the blue phase was found to be - 32 K and - 123 K for the



turquoise phase. The effective magnetic moments were found to be 1.19 and 1.948  $\mu_B / \text{Co}^{2+}$  for blue and turquoise phases respectively. Notably, susceptibility versus temperature curve for sample 6 has a maximum not present for the first four measurements of sample 4 at around 29 K indicative of the onset of 3D antiferromagnetic ordering. Assuming a low spin state for cobalt yields an effective magnetic moment of 1.73  $\mu_B / \text{Co}^{2+}$ , whilst the moment obtained for the blue phase is lower likely because of the lack of three dimensional ordering taking place yielding a lower effective magnetic moment. In literature, cobalt compounds tend to be low-spin with an increasing number of ligands surrounding the metal cation whilst the magnetic moment is expected to be slightly larger than the spin only value as calculated by equation (6).<sup>2</sup> In literature, octahedral cobalt complexes tend to be in a high spin state which does not agree with the magnetic measurements obtained.<sup>20</sup> The discrepancy between different works in literature highlights that effective magnetic moments alone are not enough to determine whether cobalt exists in a low or a high spin state. The effective magnetic moments for samples 4 and 6 were notably lower than spin-only value for  $S=3/2$  of 3.873  $\mu_B / \text{Co}^{2+}$  which does not offer a conclusive understanding of whether high spin cobalt is present in the system as other factors contribute to the effective magnetic moment such as the ligand choice.

Notably, despite the first four measurements on the blue sample giving reproducible results the fifth measurement on the blue sample shows a clear change reflected by a shallower slope than other measurements along with a higher Weiss temperature of -123 Kelvin in contrast to -32 Kelvin. After the measurement the sample changed color to turquoise suggesting that vacuum of PPMS induced a transition from blue ACC to turquoise ACC as the Weiss temperature of last measurement of 123 K is of the same order of magnitude as for the samples that were initially turquoise, 113 Kelvin.<sup>15,23</sup> Inducing a phase transition upon exposure to a vacuum is consistent with what happened to the compound when placed inside a glovebox. However, the effective magnetic moment for the transitioned blue phase of 2.452  $\mu_B / \text{Co}^{2+}$  is higher than any other measurement on either sample 4 or 6. Lastly, it is worth noting that HACC undergoes a phase transition to blue when exposed to a vacuum; hence preventing VSM from being an effective way to study the pink phase using PPMS.

According to literature in cubic halide perovskites the distortions within the crystals have an effect on the band gap. From the point of looking at the phase transition between long range ordered and disordered states, presence of static distortion raises the band gap.<sup>28</sup> Hence, it is possible that the static distortion arising from the transition from ordered blue phase to the disordered turquoise phase raises the bandgap reflected by a color change. However, it is worth noting that in the field the consensus has not been reached yet as looking through the lens of electronic structure yielded promising results for oxide-based cubic perovskites.<sup>28</sup>

Additionally, as shown in appendix 1 experiment 4 samples 4 and 6, the cell parameters for blue and turquoise are similar, though not identical, suggesting a minor structural change is present. Solving the crystal structure shows that the anilinium cations are ordered in the blue phase and disordered in the turquoise phase. Further examining the procedure used to obtain said phases selectively suggests that the volatility of propanol provided a short enough time span for the blue phase to form but not the turquoise. Whereas low volatility of hexanol has increased the crystallization time such that the material undergoes a transition whilst still dispersed in the yet-to-evaporate solvent. The latter observation suggests that lower crystallization time when using propanol yields the more kinetically stable product, blue ACC. In

contrast, longer crystallization time when using hexanol yields the more thermodynamically stable turquoise ACC.

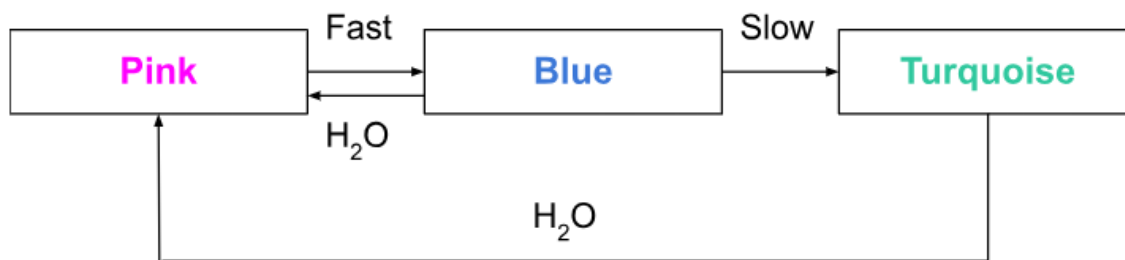


Figure 15: Diagram reflecting the order of phase transitions.

The material being photochromic, it responds to irradiation by UV inducing a phase transition from pink to blue, then to turquoise (as seen in Figure 15). As pink is the hydrated phase of ACC, transition to blue phase occurs as a result of water liberation; hence the ions rearrange to form a new favorable conformation which is blue in color.<sup>15,16</sup> Given the fact that this transition reliably occurs while undisturbed in ambient conditions implying that exposure to UV merely increases the rate at which water is released.

To probe the compound's response to temperature, samples from experiments 4 and 5 were mixed together such that there are all three phases present. Subsequently the mixed powder was spread on a glass petri dish stationed on a heating plate.

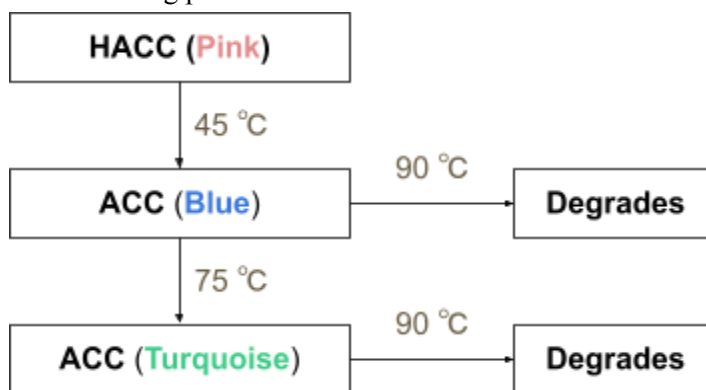


Figure 16: Diagram illustrating ACC's response to temperature

The temperature of the heating plate was gradually increased from r.t. to 105 °C over 3 hours. As illustrated in figure 16, initially only the pink phase changed from 45 °C onwards becoming blue. Upon further heating of the sample, at 75 °C the blue phase began to transition to turquoise although slowly. Once temperature reached 90 °C the sample began to degrade. Following that, an increase to 105 °C for an hour resulted in near complete degradation of the product with the color changing to a mixture of dull blue and dull green resembling neither the blue nor the turquoise phase respectively. To verify that powder has degraded, the mixture of dull blue and dull green phases was placed in a UV chamber at 20% for 1 hour which would yield a color change from blue to turquoise had the material been intact. However, despite exposing the material for a total of 2 hours to UV, there was no color change observed.



## Conclusion

The material examined in this paper is a photochromic hybrid perovskite, anilinium cobalt chloride, which upon initial examination changed color following exposure to UV radiation yielding a color change from pink to blue then to turquoise. Utilizing X-Ray Powder Diffraction, the pink phase was identified as the hydrated form of ACC whilst, blue and turquoise as anhydrous suggestive of transition between pink and blue phases being driven by release of water. Said transition is reversible as a consequence of the liberation and reincorporation of water molecules from the crystal structure inducing reorganization of the crystalline lattice forming a kinetically stable blue phase. Consequently, the thermally irreversible transition from blue to turquoise phases of a material occurs when given time or irradiation allowing the system to shift from a kinetically favored blue phase to a thermodynamically more stable turquoise phase, resulting in a more energetically favorable arrangement of the crystal lattice.

Conducting magnetic measurements with VSM on the samples shows a distinct difference in magnetic configuration between blue and turquoise phase with the latter exhibiting larger effective magnetic moment, hence stronger magnetic interactions. Despite a clear difference between the phases, both moments are closer to estimate for low spin cobalt ( $S = \frac{1}{2}$ ) with blue being lower and turquoise higher; hence the data obtained does not offer conclusive evidence on how much if any high spin cobalt is present in the material along with its potential effect on color of the product. As the blue phase underwent a transition to turquoise inside the vacuum of PPMS and the pink phase quickly underwent transition to anhydrous phase when under nitrogen conditions, measurements on the hydrated phase were not conducted as pink phase would transition to blue phase hindering the collection of data.

The change from the hydrated pink to the anhydrous state of the material is illustrative of the switch from paramagnetic to antiferromagnetic configuration. The latter state exists as blue and turquoise phases where anilinium cations are ordered or disordered respectively as hinted at by XRPD analysis. The disordered anilinium cations yield antiferromagnetic 3D ordering at low temperatures as exhibited by an increase in magnetic interactions going from blue to turquoise phase reflected by an increase in effective magnetic moment for the latter. Furthermore transitioning from ordered blue phase to disordered turquoise phase is accompanied by an increase in the band gap as a result of static distortion introduced through transition; hence a color change. Perovskites' intrinsic properties and specific peculiarities of this material make anilinium cobalt chloride a candidate for use in photochromic applications combining its ability to exhibit a color change whilst benefiting from semiconductor behavior.<sup>3,6,11,16</sup>



## Bibliography

1. Bain, G. A.; Berry, J. F. Diamagnetic Corrections and Pascal's Constants. *Journal of Chemical Education* 2008, 85 (4), 532. DOI:10.1021/ed085p532.
2. Barclay, G. A.; Collard, M. A.; Harris, C. M.; Kingston, J. V. High-Spin and Low-Spin Cobalt(II) Complexes of 8-Dimethylarsinoquinoline. *Journal of Inorganic and Nuclear Chemistry* 1969, 31 (11), 3573–3577. DOI:10.1016/0022-1902(69)80345-3.
3. Bellitto, C.; Day, P. Feature Article. Organic-Intercalated Halogenochromates(II): Low-Dimensional Magnets. *Journal of Materials Chemistry* 1992, 2 (3), 265. DOI:10.1039/jm9920200265.
4. Dandal, Y.; Bazin, C.; Pillier, F.; Cachet, H.; Pailleret, A. Influence of Chemical Conversion Parameters and Resulting PBI2 Content on Carrier Density and Morphology of the P-Type Electrodeposited Hybrid Perovskite  $\text{CH}_3\text{NH}_3\text{PbI}_3$ . *Materials Chemistry and Physics* 2023, 305, 127933.
5. Datta, S.; Limpanuparb, T. Steric vs electronic effects: A new look into stability of diastereomers, conformers and constitutional isomers 2021. DOI:10.26434/chemrxiv.13551182.v1.
6. Day, P. New Transparent Ferromagnets. *Accounts of Chemical Research* 1979, 12 (7), 236–243. DOI:10.1021/ar50139a003.
7. Dighe, A. V.; Podupu, P. K.; Coliaie, P.; Singh, M. R. Three-Step Mechanism of Antisolvent Crystallization. *Crystal Growth & Design* 2022, 22 (5), 3119–3127. DOI:10.1021/acs.cgd.2c00014.
8. Doebelin, N.; Kleeberg, R. Profex: A Graphical User Interface for the Rietveld Refinement Program BGMN. <https://journals.iucr.org/j/issues/2015/05/00/kc5013/index.html> (accessed 2024-03-22).
9. Firmansyah; Kartini, I.; Sutarno; Ruslan. Effect of Additive Polarity on the Stability of Organic-Inorganic Hybrid  $\text{CH}_3\text{NH}_3\text{PBI}_3$  Perovskite Thin Film. *Journal of Physics: Conference Series* 2021, 1763 (1), 012032.
10. Gupta, R.; Korukonda, T. B.; Gupta, S. K.; Dhamaniya, B. P.; Chhillar, P.; Datt, R.; Vashishtha, P.; Gupta, G.; Gupta, V.; Srivastava, R.; Pathak, S. Room Temperature Synthesis of Perovskite (MAPBI<sub>3</sub>) Single Crystal by Anti-Solvent Assisted Inverse Temperature Crystallization Method. *Journal of Crystal Growth* 2020, 537, 125598. DOI:10.1016/j.jcrysgro.2020.125598.
11. Hassan, Y.; Ashton, O. J.; Park, J. H.; Li, G.; Sakai, N.; Wenger, B.; Haghighirad, A.-A.; Noel, N. K.; Song, M. H.; Lee, B. R.; Friend, R. H.; Snaith, H. J. Facile Synthesis of Stable and Highly Luminescent Methylammonium Lead Halide Nanocrystals for Efficient Light Emitting Devices. *Journal of the American Chemical Society* 2019, 141 (3), 1269–1279.
12. Höcker, J.; Brust, F.; Armer, M.; Dyakonov, V. A Temperature-Reduced Method for the Rapid Growth of Hybrid Perovskite Single Crystals with Primary Alcohols. *CrystEngComm* 2021, 23 (11), 2202–2207.
13. Irie, M. Photochromism of Diarylethene Single Molecules and Single Crystals. *Photochemical & Photobiological Sciences* 2010, 9 (12), 1535–1542. DOI:10.1039/c0pp00251h.
14. Kanungo, S. B.; Mishra, S. K. Thermal Dehydration and Decomposition of  $\text{FeCl}_3 \cdot \text{XH}_2\text{O}$ . *Journal of Thermal Analysis* 1996, 46 (5), 1487–1500.





15. Lee, T.; Straus, D. B.; Xu, X.; Xie, W.; Cava, R. J. Tunable Magnetic Transition Temperatures in Organic–Inorganic Hybrid Cobalt Chloride Hexagonal Perovskites. *Chemistry of Materials* 2023, 35 (4), 1745–1751.
16. Li, X.; Chen, M.; Mei, S.; Wang, B.; Wang, K.; Xing, G.; Tang, Z. Light-Induced Phase Transition and Photochromism in All-Inorganic Two-Dimensional CS<sub>2</sub>PBI<sub>2</sub>CL<sub>2</sub> Perovskite. *Science China Materials* 2020, 63 (8), 1510–1517.
17. Liang, Z.; Tian, C.; Li, X.; Cheng, L.; Feng, S.; Yang, L.; Yang, Y.; Li, L. Organic–Inorganic Lead Halide Perovskite Single Crystal: From Synthesis to Applications. *Nanomaterials* 2022, 12 (23), 4235.
18. Mishra, S. K.; Kanungo, S. B. Thermal Dehydration and Decomposition of Cobalt Chloride Hydrate (CoCl<sub>2</sub>·xH<sub>2</sub>O). *Journal of Thermal Analysis* 1992, 38 (11), 2437–2454.
19. Momma, K. VESTA. A Three-Dimensional Visualization System for Electronic and Structural Analysis. <http://www.jp-minerals.org/vesta/en/> (accessed 2024-03-22).
20. Natarajan, C.; Palaniandavar, M. Stereochemistry of Copper (II), Nickel (II) and Cobalt (II) 2'-Hydroxy-5'-X-Chalconeoxime Complexes. *Proceedings / Indian Academy of Sciences* 1983, 92 (3), 265–270. DOI:10.1007/bf02841244.
21. Park, Y.; Song, K.; Choi, H. C. Emulsions of Miscible Solvents: The Origin of Anti-Solvent Crystallization. *CrystEngComm* 2021, 23 (4), 777–782. DOI:10.1039/d0ce01088j.
22. Physical Property Measurement System. <https://www.qdusa.com/products/ppms.html> (accessed 2024-03-08).
23. Septiany, L.; Blake, G. R. Magnetocaloric Effect and Critical Behavior in Arylamine-Based Copper Chloride Layered Organic-Inorganic Perovskite. *Journal of Magnetism and Magnetic Materials* 2022, 542, 168598. DOI:10.1016/j.jmmm.2021.168598.
24. Vraneš, M.; Gadžurić, S. B.; Zsigrai, I. J. Cobalt Halide Complex Formation in Aqueous Calcium Nitrate–Ammonium Nitrate Melts. I. Cobalt(II) Chlorides. *Journal of Molecular Liquids* 2007, 135 (1–3), 135–140. DOI:10.1016/j.molliq.2006.11.007.
25. Wang, X.; Li, X.; Tang, G.; Zhao, L.; Zhang, W.; Jiu, T.; Fang, J. Improving Efficiency of Planar Hybrid CH<sub>3</sub>NH<sub>3</sub>PBI<sub>3-x</sub>CL<sub>x</sub> Perovskite Solar Cells by Isopropanol Solvent Treatment. *Organic Electronics* 2015, 24, 205–211.
26. Xu, Y.; Hu, J.; Du, X.; Xiao, X.; Li, M.; Tang, J.; Chen, J.; He, Y. Antisolvent-assisted Crystallization of Centimeter-sized Lead-free Bismuth Bromide Hybrid Perovskite Single Crystals with X-ray Sensitive Merits. *Chemistry – An Asian Journal* 2021, 16 (24), 4137–4144. DOI:10.1002/asia.202101041.
27. Zhang, Z.; Lu, X.; Pan, F.; Wang, Y.; Yang, S. Preparation of Anhydrous Magnesium Chloride from Magnesium Chloride Hexahydrate. *Metallurgical and Materials Transactions B* 2012, 44 (2), 354–358.
28. Zhao, X.-G.; Wang, Z.; Malyi, O. I.; Zunger, A. Effect of Static Local Distortions vs. Dynamic Motions on the Stability and Band Gaps of Cubic Oxide and Halide Perovskites. *Materials Today* 2021, 49, 107–122. DOI:10.1016/j.mattod.2021.05.021.
29. Zhou, X.; Shan, J.; Chen, D.; Li, H. Tuning the Crystal Habits of Organic Explosives by Antisolvent Crystallization: The Case Study of 2,6-Dimaino-3,5-Dinitropyrazine-1-Oxid (LLM-105). *Crystals* 2019, 9 (8), 392. DOI:10.3390/cryst9080392.





## Appendix

**Appendix 1:** Table containing cell parameters refined by Profex using XRPD data obtained

| Experiment # | Sample # | Phase                    | a (Å)         | b (Å)        | c (Å)         |
|--------------|----------|--------------------------|---------------|--------------|---------------|
| 1            | 1        | ACC blue                 | 6.974±0.003   | 21.106±0.009 | 5.981±0.003   |
|              |          | HACC                     | 26.15±0.02    | 7.897±0.006  | 10.418±0.007  |
| 2            | 2        | HACC                     | 26.12±0.02    | 7.932±0.006  | 10.443±0.007  |
|              | 3        | ACC blue                 | 6.9873±0.0008 | 21.151±0.004 | 5.9833±0.0008 |
|              |          | HACC                     | 26.14±0.02    | 7.953±0.006  | 10.321±0.008  |
| 4            | 4        | ACC blue                 | 6.992±0.001   | 21.112±0.006 | 5.991±0.001   |
|              | 5        | ACC<br>(UV exposed)      | 6.996±0.001   | 21.116±0.004 | 5.9948±0.0008 |
|              | 6        | ACC turquoise            | 6.994±0.001   | 21.042±0.005 | 6.0235±0.001  |
| 5            | 7        | ACC rehydrated<br>(HACC) | 26.14±0.003   | 7.9±0.001    | 10.415±0.002  |
|              | 8        | HACC                     | 26.131±0.003  | 7.902±0.001  | 10.405±0.002  |
|              | 9        | ACC<br>(UV exposed)      | 26.10±0.03    | 7.863±0.009  | 10.36±0.004   |
|              |          | HACC<br>(UV exposed)     | 6.91901       | 20.98±0.02   | 6.002±0.004   |